ERDC/CERL TR-16-16

Construction Engineering Research Laboratory

US Army Corps of Engineers®
Engineer Research and Development Center

ERDC
INNOVATIVE SOLUTIONS for a safer, better world

DoD Corrosion Prevention and Control Program

Demonstration and Validation of a Lightweight Composite Bridge Deck Technology as an Alternative to Reinforced Concrete

Final Report on Project F09-AR16

Karl Palutke, Richard G. Lampo, Lawrence Clark, James Wilcoski, Rick Miles, and Darrel Skinner

August 2016

Demonstration and Validation of a Lightweight Composite Bridge Deck Technology as an Alternative to Reinforced Concrete

Final Report on Project F09-AR16

Richard G. Lampo and James Wilcoski

Construction Engineering Research Laboratory
U.S. Army Engineer Research and Development Center
2902 Newmark Drive
Champaign, IL 61822

Karl Palutke, Lawrence Clark, Rick Miles, and Darrell Skinner

Mandaree Enterprise Corporation (MEC)
812 Park Drive
Warner Robins, GA 31088

Final report

Prepared for Office of the Secretary of Defense (OUSD(AT&L))
3090 Defense Pentagon
Washington, DC 20301-3090

Under Project F09-AR16, "Demonstration and Validation of a Lightweight Composite Bridge Deck Technology as an Alternative to Reinforced Concrete"

Abstract

Cyclic loading and weathering of reinforced concrete bridge decks cause corrosion of reinforcement steel, which leads to cracking, potholes, and other problems. This project demonstrated the use of a glass-fiber reinforced polymer (GFRP) composite deck system, which does not use any reinforcement steel, on a deteriorated concrete bridge at Redstone Arsenal, AL. A pultruded deck system made by Zellcomp, Inc., was selected for demonstration and validation. The demonstrated system was designed to retain the 36-ton (HS-20) load rating of the original bridge. This report documents demolition of the existing deck, installation of the composite deck system, materials and load testing, remediation of initial problems, and an economic analysis in terms of return on investment (ROI).

The main problems identified after construction were reflective cracking of the polymer-concrete wear surface applied over the composite deck sections; and gaps and voids related to grout forms and supports installed between bridge girders and deck sections. After repairs, the bridge was returned to service and is functioning normally. The calculated ROI for this technology was 5.4. Although there are not yet consensus standards for composite bridge decks, the demonstrated technology can be effectively applied using existing load-resistance design factors and manufacturer installation instructions.

Contents

Figures and Tables

Figures

Tables

Preface

This demonstration was performed for the Office of the Secretary of Defense (OSD) under Department of Defense (DoD) Corrosion Control and Prevention Project F09-AR16, "Demonstration and Validation of a Lightweight Composite Bridge Deck Technology as an Alternative to Reinforced Concrete." The proponent was the U.S. Army Office of the Assistant Chief of Staff for Installation Management (ACSIM), and the stakeholder was the U.S. Army Installation Management Command (IMCOM). The technical monitors were Daniel J. Dunmire (OUSD(AT&L)), Bernie Rodriguez (IMPW-FM), and Valerie D. Hines (DAIM-ODF).

The study was performed by the Engineering and Materials Branch of the Facilities Division (CEERD-CFM), U.S. Army Engineer Research and Development Center, Construction Engineering Research Laboratory (ERDC-CERL), Champaign, IL. Significant portions of the work were executed by Mandaree Enterprise Corporation and its subcontractors, Zellcomp, Inc.; Angelo Iafrate Construction Company; and Bridge Diagnostics, Inc. At the time this report was prepared, Vicki L. Van Blaricum was Chief, CEERD-CFM; Donald K. Hicks was Chief, CEERD-CF; and Kurt Kinnevan, CEERD-CZT, was the Technical Director for Adaptive and Resilient Installations. The Deputy Director of ERDC-CERL was Dr. Kirankumar Topudurti, and the Director was Dr. Ilker Adiguzel.

The Commander of ERDC was COL Bryan S. Green, and the Director was Dr. Jeffery P. Holland.

Executive Summary

Cyclic loading and weathering of reinforced concrete bridge decks result in moisture and chloride penetration of the concrete. These processes corrode reinforcement steel, which accelerates bridge degradation to cause cracking, potholes, and other safety problems. This project demonstrated the use of a glass-fiber reinforced polymer (GFRP) composite deck system that does not use any steel reinforcement elements. The technology was demonstrated on Bridge 18 at Redstone Arsenal, AL, a one-way, one-lane bridge on Morris Road that overpasses and leads to an on-ramp to Toftoy Road. The bridge measures 20 ft wide (curb to curb) and 198 ft, 9 in. long, and it has a load rating of 36 tons. Significant portions of steel and concrete were deteriorating at the time of the demonstration.

The replacement composite deck system was designed to retain the original 36 ton (HS-20) load rating. A pultruded deck system made by Zellcomp, Inc., Durham, NC, was selected as the low cost-option. This system does not use any field-applied adhesives like some other composite deck systems. The composite deck is topped with a polymer concrete roadway wear surface that is applied over the pultruded deck sections. Before the replacement deck was put into service a load-capacity test was performed, deck system materials were lab-tested to verify performance, and atmospheric corrosivity of the location was tested.

After several months of use, reflective cracking of the wear surface was observed, a problem sometimes seen with other composite deck designs. The cracks were repaired, as were some other problems related to installation. The bridge is currently open for traffic and functioning as expected.

GFRP composite bridge deck systems offer benefits of being corrosion resistant and lightweight (reduced dead load). It can be installed faster than reinforced concrete, allowing a bridge to be put back into service quicker than with a conventional deck. A major barrier to more widespread use is the lack industry consensus standards for composite bridge deck systems. However, applicable American Association of State Highway and Transportation Officials (AASHTO) load and resistance design factors can be applied in conjunction with deck manufacturer installation and maintenance guidance to specify this technology on military installations.

Unit Conversion Factors

Multiply	By	To Obtain
degrees Fahrenheit	(F-32)/1.8	degrees Celsius
feet	0.3048	meters
inches	0.0254	meters
gallons (U.S. liquid)	3.785412 E-03	cubic meters
ounces (U.S. fluid)	2.957353 E-05	cubic meters
pounds (mass)	0.45359237	kilograms
pounds (force) per square inch	6.894757	kilopascals
square feet	0.09290304	square meters

(This page intentionally blank.)

1 Introduction

1.1 Problem statement

A well-maintained road network on a military installation is central to the success of its mission, operations, and security. The condition of bridges is particularly important: they are necessary for traversing unavoidable obstacles (e.g., waterways, ravines, other transportation infrastructure), and there is usually no simple way to detour around them when closed to address traffic safety issues.

Bridge deck corrosion is a large and growing problem for the nation's transportation networks. The Federal Highway Administration (FHWA) Report RD-01-156 [Ref. 1] states that maintenance and capital costs for concrete decks account for approximately one quarter of the direct costs associated with bridge corrosion. Additionally also reports that indirect costs to bridge users, in the form of traffic delays and lost productivity, can amount to ten times the direct costs of the actual deck deterioration. According to the Illinois and New York state departments of transportation—two states where road salts are used extensively for deicing—the average service life of a steel-reinforced concrete bridge deck is 25 years. [Ref. 2]. The condition of bridges on military installations reflects this same situation, with many in urgent need of major repairs or replacement due to corrosion and materials degradation. More than 80% of the Army's bridges are concrete or steel, with the vast majority having reinforced concrete decks.

On 1–2 May 2008, a meeting titled "Workshop on Structural Health Monitoring and Corrosion Degradation Modeling" was held in Arlington, VA, in support of the Department of Defense (DoD) Corrosion Prevention and Control (CPC) Program. Attending experts from Army, Navy, government, industry, and academia recognized deterioration and failure of bridge decks as the top problem and maintenance requirement for bridges. Design and construction problems, in combination with exposure to the environment, result in cracking and spalling of the concrete and corrosion of the steel reinforcement bar (rebar). Bridges in regions where salts are applied to remove winter ice and in coastal areas exposed to splash-zone seawater are degraded more quickly and severely. Inadequate coverage of the

rebar due to cracking and other problems allow salts to attack the steel and cause concrete spalling (Figure 1). The loss of concrete exposes more steel, further accelerating corrosion until the bridge becomes unsafe, and costly repairs are needed. When a deteriorated deck is repaired with an overlay or is rehabilitated using the same materials, the degradation cycle may be slowed but not halted.

Figure 1. Spalling on underside of original Bridge 18 deck.

Glass fiber-reinforced polymer (GFRP) composite bridge decks offer many advantages over steel-reinforced concrete decks. A GFRP composite bridge decks is typically only 10%–20% the weight of a structurally equivalent reinforced concrete deck, which significantly reduces dead load and makes it possible to rehabilitate older bridges to their original design loads. Because GFRP composites are not susceptible to metallic corrosion, these materials offer a promising alternative to conventional steel-reinforced concrete materials in this highly demanding application. Corrosion-resistant GFRP thermoset composite bridge decking systems may provide low-maintenance service for an estimated 75 years [Ref 1]. They have the

potential to greatly reduce maintenance costs and assure long-term operation at potentially higher load capacity at a lower life-cycle cost compared to reinforced concrete and steel decks.

The Army has more than 1,500 vehicle bridges on its installations. Premature bridge deck failures on installations can compromise mission effectiveness and inflate infrastructure costs. Personnel at Redstone Arsenal, AL, identified several small steel bridges needing extensive deck repair or complete replacement. One Redstone bridge was selected from the Army bridge inspection database as the subject of a CPC project in which a severely degraded deck would be replaced with a commercially available GFRP composite decking system.

1.2 Objective

The objective of this project was to demonstrate and validate the performance and cost of a GFRP composite bridge deck system used to rehabilitate a deteriorated reinforced-concrete vehicle bridge at Redstone Arsenal.

1.3 Approach

Bridge 18, which is located on Morris Road and crosses the Toftoy Throughway, was selected for the demonstration (see Figure 2). The deteriorated concrete deck was demolished, and preparations were carried out to replace it with the GFRP system described in the main text.

Figure 2. Original Morris Road bridge deck (Bridge 18), showing concrete spalling at right.

In preparation for this work, the Redstone Arsenal Directorate of Public Works (DPW) rehabilitated the four steel girders supporting the span and replaced the bridge's bearing pads. After installation of the deck, the DPW modified both approaches to accommodate the new deck surface.

After construction was completed, a load test was performed to test deck displacement and strain relative to the design requirements. Also, laboratory testing of GFRP composite specimens, sampled from the same lot as the deck panels, was performed prior to deck installation. In addition to the standard tests, additional specimens were subjected to accelerated aging tests (see section 3.1). Finally, metallic atmospheric corrosion coupons were placed at the bridge site, retrieved quarterly, and tested for mass loss and surface chloride content. This testing was done to characterize the relative corrosivity of the local environment at the installation site.

1.4 Scope

In addition to describing the installation and testing of the composite deck system, this report documents follow-up assessments and work performed to address several significant issues related to the wear surface and drainage that were identified by DPW personnel shortly after the rehabilitated

bridge was reopened to traffic. The repairs are discussed in section 3.2.3, and lessons learned from this work are summarized in section 3.3.1.

2 Technical Investigation

2.1 Project overview

2.1.1 Fabrication process

Pultrusion is a process for manufacturing composite materials with a constant cross-sectional profile. In the pultrusion process, reinforcing fibers are pulled through a resin and then through a heated mold, inside of which the resin polymerizes, fixing the shape of the material. For this project, E-glass reinforcing fibers and an isophthalic polyester resin were used to produce a GFRP composite.

The project team evaluated pultruded structural products from three suppliers. All three were judged to be technically acceptable. The system from Zellcomp, Inc. (Durham, NC) was selected as the low-cost option.

2.1.2 Specifications

The GFRP composite deck was designed to comply with the American Association of State Highway and Transportation Officials (AASHTO) load and resistance factor design specifications [Ref. 3, with 2008 interim revisions]. The design live load was AASHTO HS-20 vehicle plus impact. The design was compliant with bridge details shown in Alabama Department of Transportation (ALDOT) Standard Drawing I-131 [Ref. 4]. The shear studs were designed to be installed in accordance with Nelson welding specification S3L.*

2.1.3 Application design details

Bridge 18 is 200 ft long, 20 ft wide, and one lane wide. The base deck section consists of 77 individually pultruded composite panels mechanically fastened together at lap joints. Each individual panel is 6.5 in. thick and 21 ft, 8 in. wide. The length of the panels varies between 1 ft, 9.5 in. and 2 ft, 7 in. A typical cross-section of the GFRP composite panels is shown in Figure 3. (The figures for this chapter appear immediately after the conclusion of the text.) A cross-sectional drawing of the bridge with the composite deck installed on the bridge girders is shown in Figure 4. The

* Nelson Stud Welding, Inc., Elyria, OH.

deck is designed with 0.5 in. weep holes to drain the interior channels where water may collect.

The deck system also includes flat GFRP composite sheets, which are attached on top of the extruded panels to provide a substrate for the application of a wear surface. The flat sheets measure 4 ft wide and 0.5 in. thick. Length varies from 10 ft, 7.5 in. to 7 ft, 1.5 in. The design requires 80 sheets, installed in a staggered pattern. The sheets are attached to the extruded panels with 410 stainless steel ASTM A493 [Ref. 5] self-drilling hex washer-head screws.

In order to provide uniform support of the composite deck over the bridge girders, a grout form was designed for installation on top of each girder before the deck was installed. The form allows for the pouring of a grout haunch over each girder to provide this support. The deck sections are aligned over the grout forms and drilled with 3 in. diameter access holes through which the shear stud is inserted and welded, and into which grout will flow from channels in the pultruded section into the form below. Before applying the grout, foam dams are inserted into the pultruded sections parallel and adjacent to the studs and access holes to create pockets. These foam dams direct the grout into the access holes and prevent it from completely filling the channels in the pultruded section. The grout flows from the pultrusion down into the form, curing into a haunch that serves as a contact pad and anchorage for the composite deck sections.

In order to protect the bridge ends from impacts or other damage, they are covered with a right-angle steel plate fabricated from ASTM A709 grade 36 steel [Ref. 6] and galvanized in accordance with ASTM A123 [Ref 7]. The plates are 0.5 in. thick and overlap the top of the deck by 14 in. In addition, the channels of the first pultruded deck section on each end were filled with concrete to add stiffness.

Barrier rails are attached to the two outermost girders. The section of the girders complies with ALDOT Standard Drawing I-131 [Ref. 4]. A cross-section of the barrier rail is shown in Figure 5.

The GFRP composite top sheets are protected with a 0.5 in. thick wear surface made of a polymer concrete material called Flexolith.* This two-part

* Euclid Chemical Co., Cleveland, OH.

epoxy is mixed and spread to 0.25 in. thick, and then aggregate is sprinkled onto it before it sets. After the first layer sets, a second layer is added using the same procedure.

In order to facilitate drainage and prevent runoff from the edges of the bridge to the highway below, six scuppers (three at each end) are installed through the bridge deck. The scuppers are attached to drainage plumbing provided by Redstone Arsenal DPW.

2.2 Installation

Installation began with demolition of the existing bridge deck and barrier rails using concrete saws. This operation is shown in Figure 6 and Figure 7. Next, the barrier rails were removed (Figure 8). Finally, the bridge deck was removed in sections (Figure 9).

Next the girders were cleaned, inspected and rehabilitated. The inspection revealed that the upper corners of the girder ends needed to be replaced due to extensive corrosion. Figure 10 through Figure 12 show an end of a girder with the section removed, the extent of corrosion damage, and the repaired girder. Also the southeastern-most girder section was replaced in its entirety due to corrosion and impact damage. All girder refurbishment was performed by Redstone Arsenal DPW and was not part of the CPC project.

After the girders were refurbished or replaced, the forms for the grout haunch were installed. These were fabricated using 0.125 in. thick steel set upright and tack welded around the perimeter of the top surface of the girder to create a form to hold the liquid grout (Figure 13). (For this bridge, the grout haunch was a minimum thickness of 2.75 in. in order to clear rivets used in the girder connections.) After the grout form was constructed, the pultruded deck sections were placed directly on top of the welded grout form. The deck sections were placed by hand, progressively providing a work surface for transporting the new sections over the previously placed sections using a pallet jack (Figure 14). The deck is shown in Figure 15 with all pultruded sections in place.

Next, workers drilled 3 in. diameter holes (Figure 16) in each deck section to allow for welding the shear studs in place and to serve as grout-injection points. Typical access holes are shown in Figure 17. At this same time, the 0.5 in. weep holes were drilled into the deck sections.

Once the access holes were drilled, shear studs were welded to the girders using a specialized welder and gun system designed to perform in confined locations (Figure 18). The stud was loaded into the gun, placed into the desired location, and the weld completed when the trigger was pulled (Figure 19).

After the shear studs were welded in place, the grout form was prepared for pouring. All joints between the steel form, the girder below, and the deck above were caulked using Tremco TremPro 626 sealant. Due to the age of the girders (approximately 45 years in service) and the slope of the bridge, there were gaps between the form and bridge deck that were too large to be filled with caulk alone. In those cases, a 5/8 in. foam backing rod was inserted into the gap before caulking. The caulking process is shown in Figure 20, and some typical finished joints are shown in Figure 21. After the caulking was complete, the grout pockets were created in pultruded sections by placing foam dams in channels parallel to the shear stud/grout access holes (Figure 22).

Next, Euclid NS Grout from Euclid Chemical was mixed in accordance with the manufacturer's instructions. Because the haunch was deeper than 2 in., the manufacturer required that pea gravel aggregate be added to the grout as a thermal stabilizer. Grout was mixed with a portable mixer and added to the pockets using small buckets (Figure 23). Mechanical vibration was applied to facilitate grout flow, as shown in Figure 24. Grout was applied in one pocket until it filled the trough underneath and rose into the adjacent pocket. At this point, the application pocket was topped off and application resumed in the adjacent pocket. Completed grout pockets are shown in Figure 25. Also, the bottom panels on either end were filled with concrete. Some concrete fill is visible in Figure 26, which shows an end section as it appeared after the completion of the next step.

After the concrete fill of end sections was completed, the top sheets were attached. A chalk line was used to establish the bridge centerline (Figure 27), and the center row of top sheets was aligned with it (Figure 28 and Figure 29). Sheets were added progressively outward from the center row. Fastener holes were drilled before the sheets were placed, as shown in Figure 30. The installation and completed top layer of GFRP composite sheets are shown in Figure 31 and Figure 32. Scuppers were then installed through the top sheet, as shown in Figure 33. Finally, the metal end plates

were installed to protect the composite deck components from vehicle wheel impacts. Installation of a plate is shown in Figure 34.

The barrier rail was installed by first constructing the steel reinforcement and then building plywood forms to contain the concrete (Figure 35 and Figure 36). To accommodate saw-cut expansion joints without exposing the steel reinforcement, the steel was precut to create a 4 in. gap at the planned locations of the joints before the concrete pour. This is shown in Figure 37. The concrete pour is shown in Figure 38. After the concrete set, the forms were removed and the surface of the barrier rail was finished (Figure 39). The finished and cured barrier rail with an expansion joint is shown in Figure 40.

The final step in construction of the bridge deck was the installation of the polymer concrete wear surface. The two components of the polymer matrix were mixed as shown in Figure 41. Once the mixing was complete, it was spread onto the surface (Figure 42). Before the matrix set, aggregate was broadcast to complete the concrete material and provide the desired texture (Figure 43). After the matrix set, a second layer of material was applied over the entire surface (Figure 44).

The completed bridge is shown in Figure 45 and Figure 46. Completed details are shown from various perspectives in Figure 47 through Figure 53.

2.3 In-service monitoring and initial deck performance issues

Before the bridge was opened to traffic, a one-time load test was conducted on 25 March 2010. Strain and displacement gauges were temporarily installed at several points on the bridge, and the test was conducted with a vehicle that approximated a HS-20 load. The results were judged to indicate that the bridge was safe for vehicular traffic. (Load test details are given in Chapter 3.) After the load test was concluded and construction on the bridge deck finished, a contractor working for the Redstone DPW refurbished the roadway and guardrail approaches to the bridge.

The bridge was opened to traffic in May 2010. However, in October 2010, Redstone DPW personnel notified the Engineer Research Development Center, Construction Engineering Research Laboratory (ERDC-CERL) about several problems observed with the bridge.

The first problem was that cracks had developed in the wear surface. It quickly became apparent that they were reflective cracks, as their location coincided with the joints between the composite cover sheets over the bridge deck. An example of this cracking is shown in Figure 54, which has been visually enhanced to highlight the cracks.

The second problem was that voids were discovered in the grout haunch between the girders and the bottom of some pultruded deck panels. In several areas near the southwest end of the bridge, the voids were large enough to leave the deck locally unsupported. The gap left by one of the voids is visible in Figure 55, which also has been contrast-enhanced to help show the dark shadow between the bottom of the deck and the steel form and girder. Also visible in the figure is the location where strain and displacement gauges were installed for the load test. It is worth noting that the bridge deck exceeded its performance requirements relative to strain and displacement despite the proximity of the strain and displacement gauges to one of the isolated areas lacking full structural support.

The third reported problem was that moisture was clearly migrating inside the deck panels and collecting on the steel girders. At several locations, water was visibly collecting on the grout forms and girders, then dripping onto the bridge abutment or the road surface. This phenomenon is also visible in Figure 55.

During an inspection in December 2010, MEC noticed two additional issues with the wear surface and deck. First, two of the GFRP composite top sheets had become loose and were no longer flush with the adjacent sheets. Second, the wear surface adjacent to one of the sheets had failed, and the sheet was visible and unprotected. Both problems are shown in Figure 56. The edge of the composite sheet adjacent to the scale is clearly visible in the figure, as is the top surface of the adjacent sheet.

Remediation of these issues is discussed in Chapter 3.

2.4 Figures for Chapter 2

Figure 3. Cross section of Zellcomp composite deck panel.

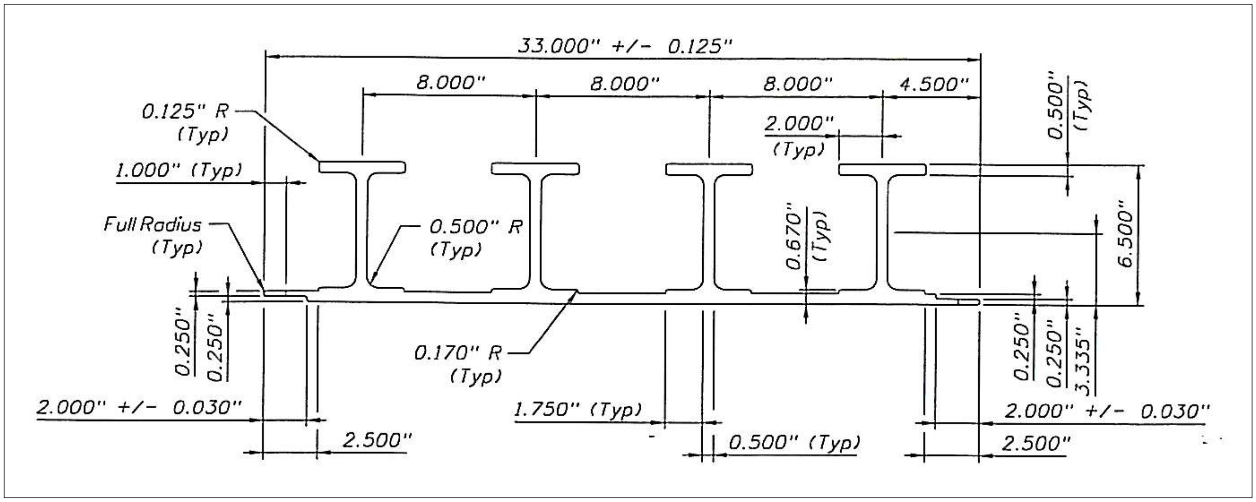

Figure 4. Cross-sectional drawing of bridge with composite deck installed on bridge girders.

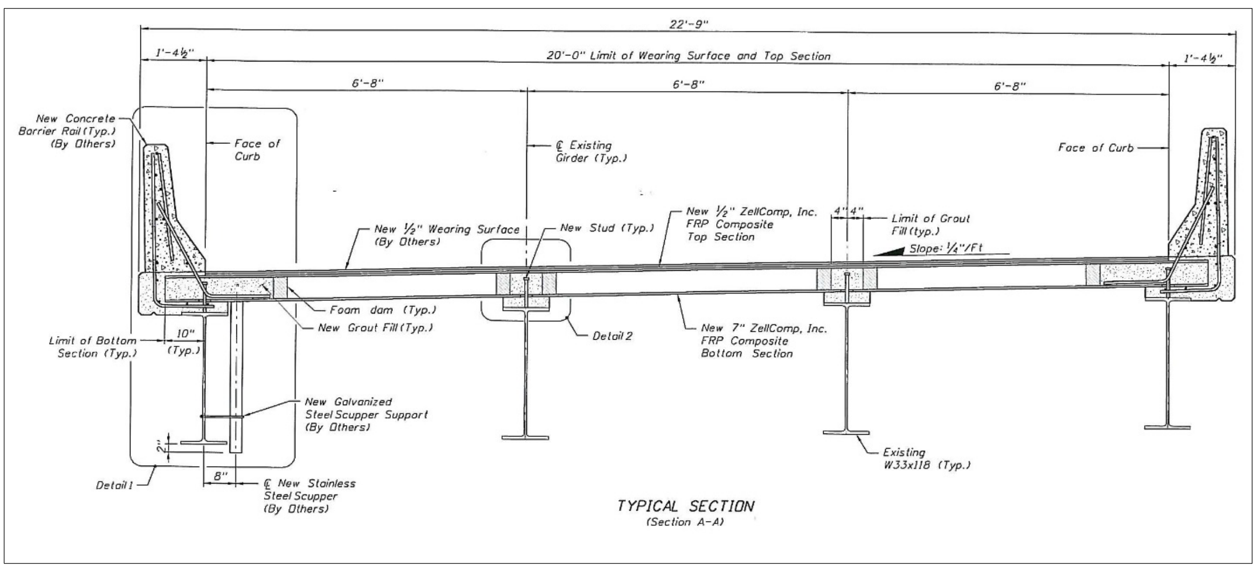

Figure 5. Details of barrier rail cross-section (from Detail 1, lower left in Figure 4).

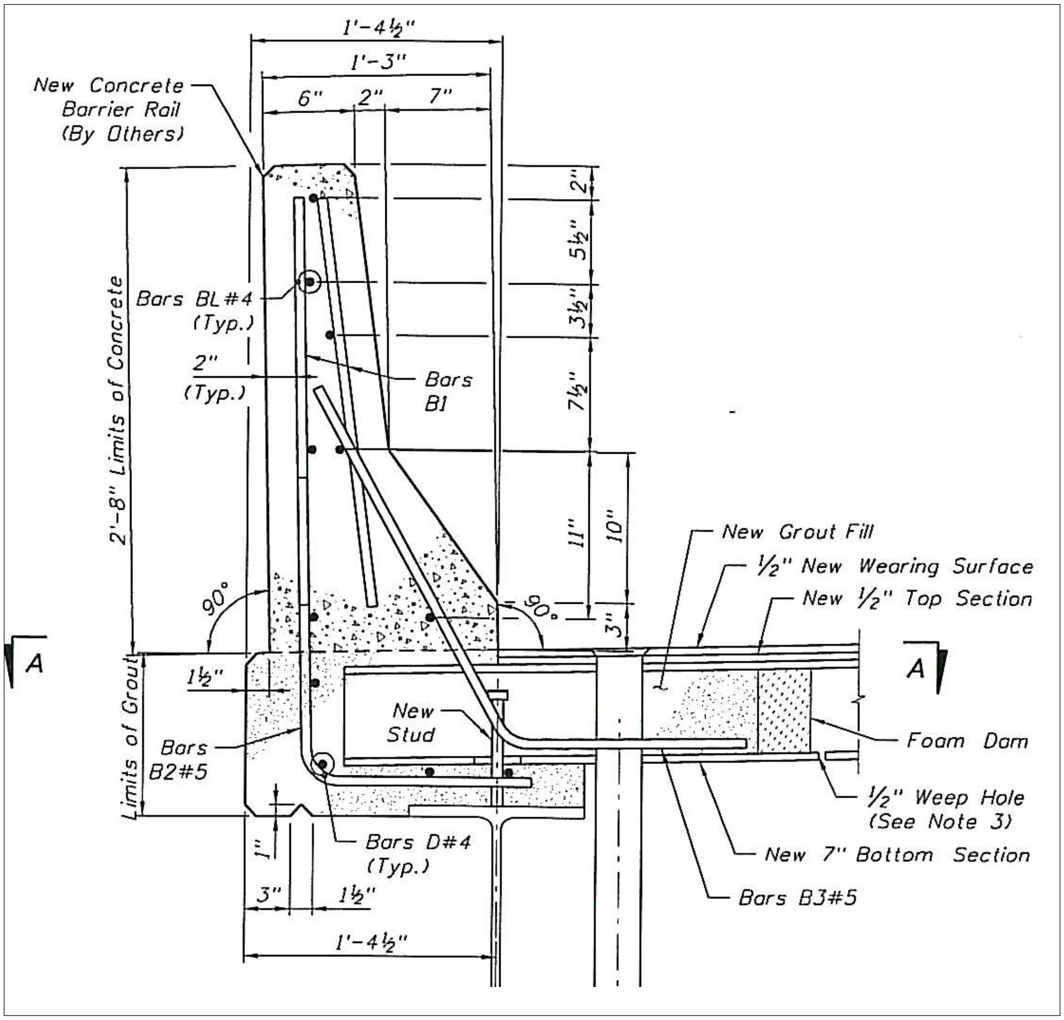

Figure 6. Cutting original bridge deck and barrier rail during demolition.

Figure 7. Sectioning of barrier rail.

Figure 8. Removal of barrier rail section.

Figure 9. Removal of concrete deck section.

Figure 10. Girder with corroded section removed.

Figure 11. Removed section of girder shown in Figure 10.

Figure 12. Repaired section of girder shown in Figure 10.

Figure 13. Form for grout haunch fabricated by tack welding steel strips to the top of the girder.

Figure 14. Placement of pultruded deck sections on top of the grout haunch form.

Figure 15. All pultruded deck sections in place over grout forms on girders.

Figure 16. Drilling access hole in pultruded section.

Figure 17. Drilled access holes shown before stud installation.

Figure 18. Shear stud welding head and gun with stud loaded.

Figure 19. Welding a shear stud.

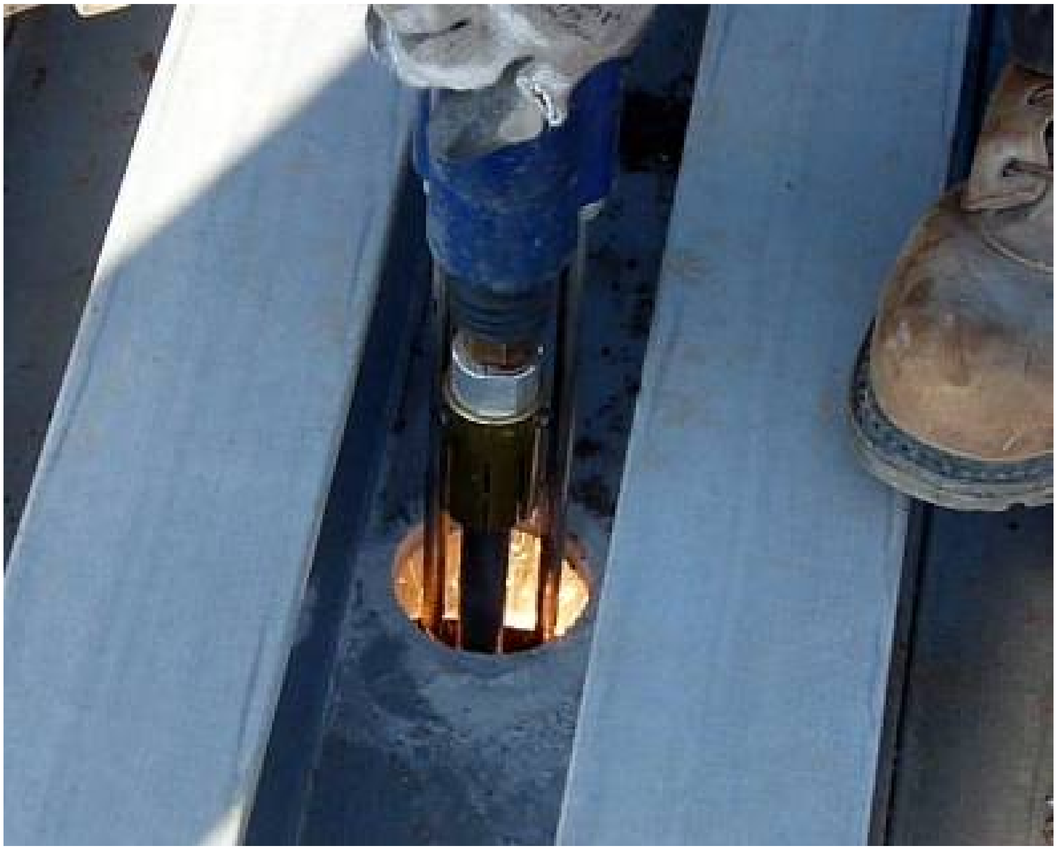

Figure 20. Caulking gaps above and below grout form.

Figure 21. Caulked grout form (between girder flange and bottom of deck).

Figure 22. Foam grout dams in pultruded deck section.

Figure 23. Hand-pouring grout into grout pockets.

Figure 24. Vibrating fluid grout.

Figure 25. Filled grout pockets.

Figure 26. Concrete-filled bridge end showing sheet screwed to pultruded section.

Figure 27. Bridge deck centerline.

Figure 28. Centering GFRP composite top sheet.

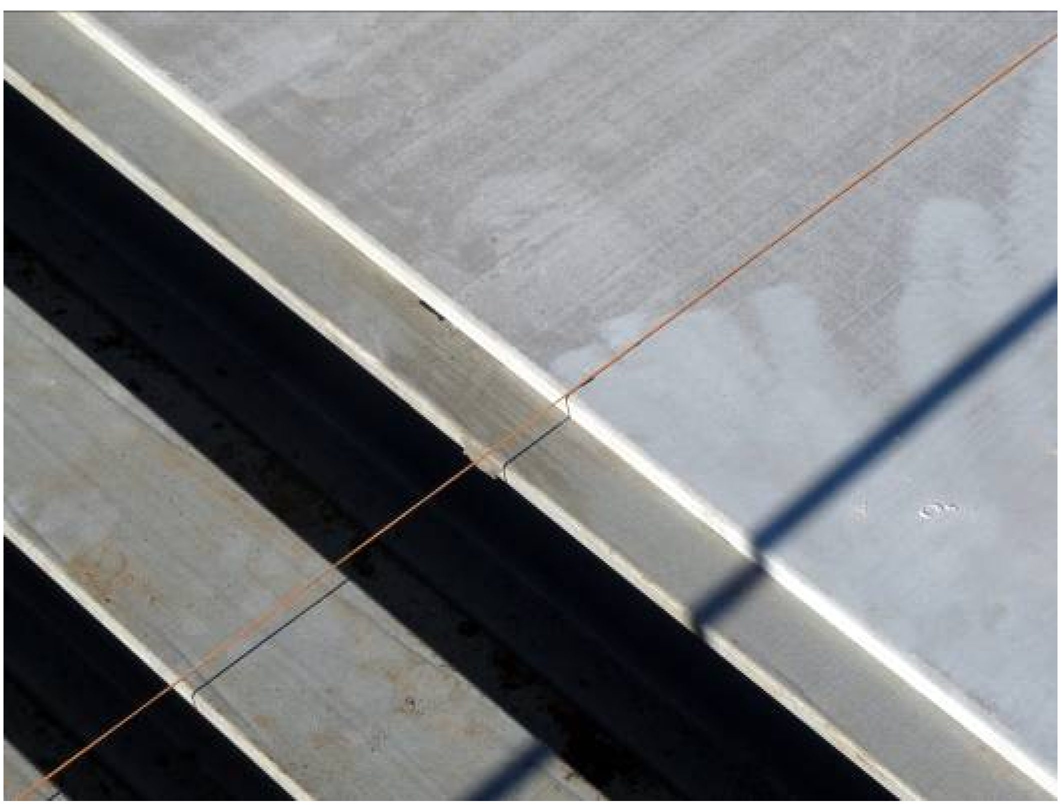

Figure 29. Centered GFRP composite top sheets.

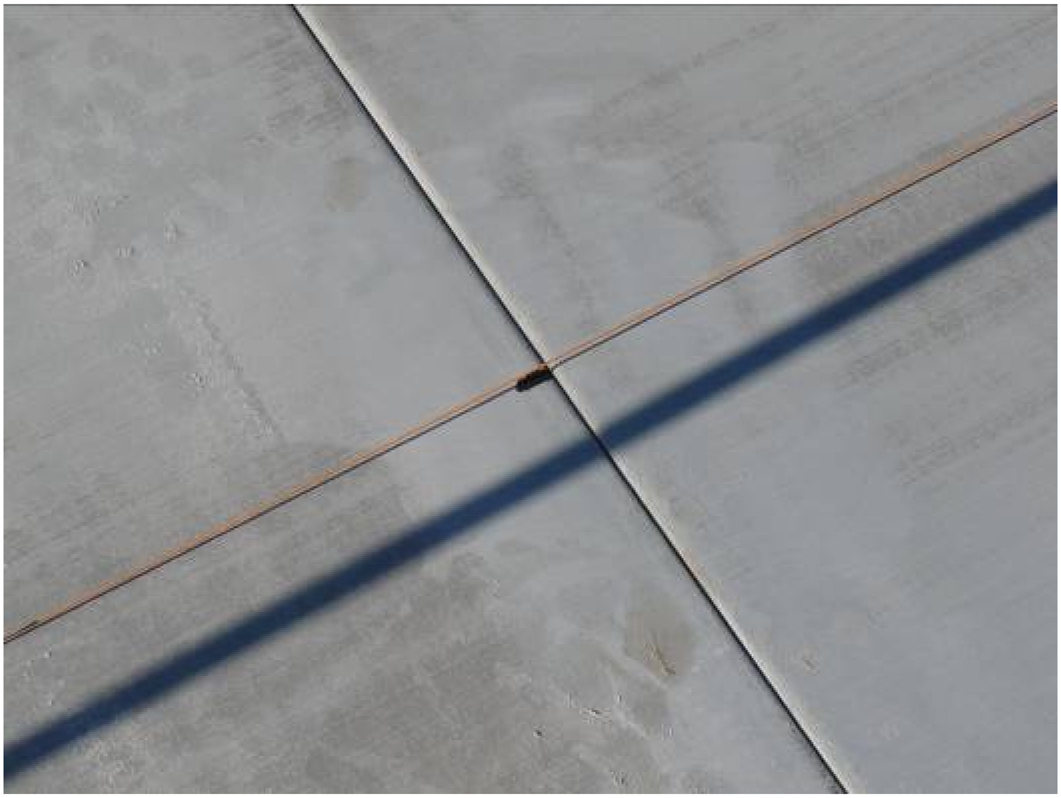

Figure 30. Holes drilled in GFRP composite top sheet before attachment with screws.

Figure 31. Installation of GFRP composite sheets.

Figure 32. Installed GFRP composite top sheets.

Figure 33. Scuppers installed in top sheet
before barrier rail and wear surface installation.

Figure 34. Installation of metal impact plate on end of deck.

Figure 35. Barrier rail reinforcement steel in place.

Figure 36. Barrier rail reinforcement and formwork.

Figure 37. Cuts in barrier rail reinforcement steel for concrete expansion joint.

Figure 38. Barrier rail concrete pour into formwork.

Figure 39. Finished barrier rail.

Figure 40. Cured barrier rail with saw-cut expansion joint.

Figure 41. Mixing two-part polymer for wear surface.

Figure 42. Application of polymer material.

Figure 43. Broadcasting aggregate to complete polymer concrete.

Figure 44. Application of second coat of polymer.

Figure 45. Completed bridge in service.

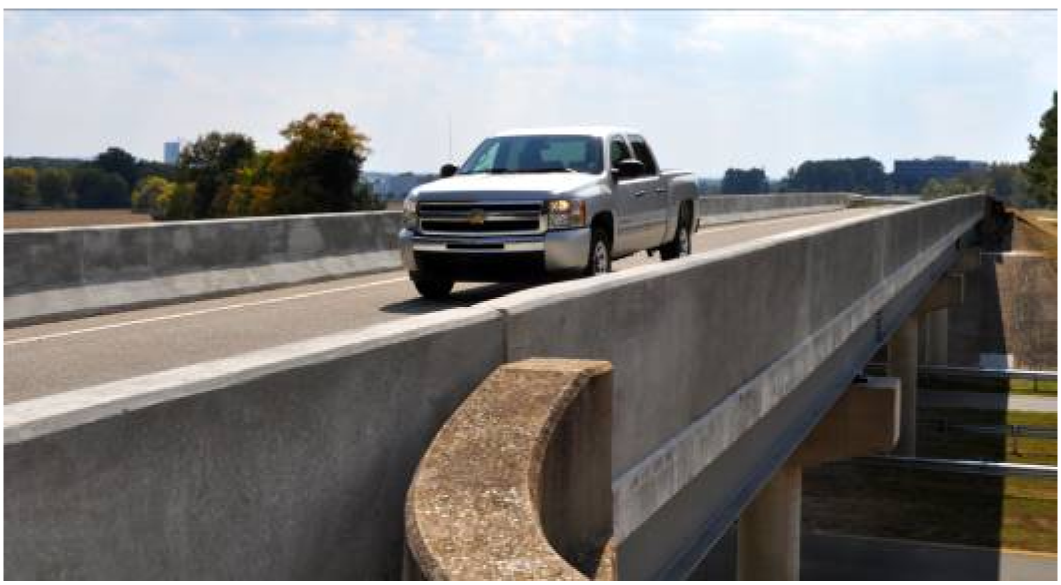

Figure 46. Completed bridge, showing girders and concrete barrier.

Figure 47. Completed wear surface and new approach.

Figure 48. Completed wear surface.

Figure 49. Barrier rail transition on bridge approach.

Figure 50. Expansion joint between new approach (left) and bridge deck.

Figure 51. Finished scuppers.

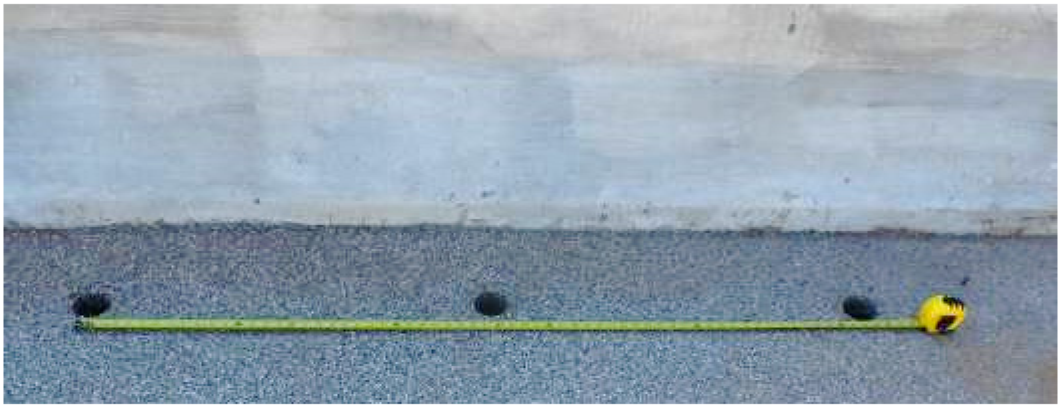

Figure 52. Finished scupper plumbing.

Figure 53. Approach detail.

Figure 54. Wear surface cracks (contrast enhanced).

Figure 55. Deck gap over steel and signs of unwanted drainage (contrast enhanced).

Figure 56. Raised GFRP composite sheet and damaged wear surface.

3 Discussion

3.1 Metrics and material-testing protocols

3.1.1 Composite deck material

The GFRP material used to fabricate the bridge deck was tested before the deck was installed. Test samples were taken from actual deck sections fabricated for the Bridge 18 production run. Samples were tested for flexural strength and flexural modulus in accordance with ASTM D790-10, *Standard Test Methods for Flexural Properties of Unreinforced and Reinforced Plastics and Electrical Insulating Materials* [Ref. 8]. For tensile strength and tensile modulus, the samples were tested in accordance with ASTM D638-10, *Standard Test Method for Tensile Properties of Plastics* [Ref. 9].

Identical material coupons were also sent to a testing laboratory for an accelerated exposure test series as follows.

Five coupons were exposed to ultraviolet A (UVA) 340 radiation for 2,000 hours in accordance with ASTM G151-10, *Standard Practice for Exposing Nonmetallic Materials in Accelerated Test Devices that Use Laboratory Light Sources* [Ref. 10]; ASTM G154-12, *Standard Practice for Operating Fluorescent Ultraviolet (UV) Lamp Apparatus for Exposure of Nonmetallic Materials* [Ref. 11]; and ASTM D4329-13, *Standard Practice for Fluorescent Ultraviolet (UV) Lamp Apparatus Exposure of Plastics*, Procedure 7.2.2, Cycle B [Ref. 12]. With typical irradiance at 340 nm of 0.77 W/(m^2 nm), this cycle is as follows:

- eight hours UVA with uninsulated black panel temperature controlled at 70 °C, and
- four hours condensation (no light) with uninsulated black panel temperature controlled at 50 °C.

Six coupons were subjected to a 3% solution of salt water (dissolving 3 parts sodium chloride in 97 parts water by mass) exposure cycle to determine the effect of this exposure on the mechanical properties of the specimens. A four-sided acrylic glass dam was fabricated slightly smaller than the face of the specimen. The height of the dam was sufficient to contain a solution depth of 1.5 in. Silicone caulk was used to secure and seal the dam from the outside edges to one face of the specimen. A loose-fitting cover

was used to minimize evaporation. The dams were filled with the 3% salt solution and left covered at standard room temperature (73 °F ± 5 °F) and humidity (50% ± 5%) for two weeks. After two weeks, the dams were emptied, and the specimen was allowed to dry for two weeks. At the end of the two weeks drying time, three of the specimen dams were refilled with the 3% salt solution. The dam was removed from the other three specimens. For the three specimens re-exposed to the salt solution, the solution was emptied after two weeks of additional exposure at standard conditions. The specimens were allowed to dry, and the dams were removed. All exposed specimens were then tested in accordance with ASTM D3039-08, *Standard Test Method for Tensile Properties of Polymer Matrix Composite Materials* [Ref. 13].

3.1.2 Atmospheric coupons

Assessment of atmospheric corrosion in the demonstration area was made using a test rack of coupons made from silver, copper, 1010 steel, and three aluminum alloys—2024 T3, 6061 T6, and 7075 T6. The dimensions for the metal coupons were 1 x 4 x 1/16 in. The metal coupons were mounted on a polymer sample card using nonmetallic fasteners that suspend the samples 0.25 in. away from the card. The metal coupons were not in contact with each other. One set of coupons was removed every three months and analyzed for mass loss in accordance with ASTM G1-03, *Standard Practice for Preparing, Cleaning, and Evaluating Corrosion Test Specimens* [Ref. 14]. Atmospheric chloride testing was done in accordance with ASTM B825-08, *Standard Test Method for Coulometric Reduction of Surface Films on Metallic Test Samples* [Ref. 15].

3.1.3 Load testing

Finally, bridge deflection and strain were tested onsite (see section 3.2.1) and compared to the design displacement requirement (i.e., less than L/500, where L is the distance between the centerline of adjacent girders). For this bridge, the girders are spaced every 80 in. on center, requiring a displacement of less than 0.16 in. For the strain, the requirement was that the maximum strains not exceed 10% of the maximum allowable strain. This produces a maximum strain limit of 3,220 microstrain ($\mu\varepsilon$).

3.2 Results

3.2.1 Test results

3.2.1.1 Composite deck material

The initial material testing was conducted by Creative Pultrusions, Inc. (Alum Bank, PA), as part of the manufacturing process for the deck. Specimens were cut from sections of decking manufactured as part of the production run for this project. The tensile and flexural properties were tested by an independent laboratory according to the methods cited above, and the results are shown in Table 1. The full results are shown in Appendix A.

Table 1. Initial GFRP composite property testing results.

Property	Test	Average	Std. Deviation	Units
Tensile Strength Lengthwise	D638	45,304	2,685	psi
Tensile Modulus Lengthwise	D638	4.32E+06	2.37E+05	psi
Flexural Strength Lengthwise	D790	44,760	3,113	psi
Flexural Modulus Lengthwise	D790	2.78E+06	2.31E+05	psi

Twelve coupons were sent for accelerated aging as described in section 3.1. The results of the UVA exposure tests are shown in Table 2, and the results of the salt exposure tests are shown in Table 3. After the UVA exposure, the average tensile strength decreased by 18% (from 45,304 psi to 36,957 psi), while the elastic modulus decreased by 6% (from 4,320,000 psi to 4,073,333 psi). For the specimens exposed to salt water for two weeks, the tensile strength decreased by 19% (from 45,304 psi to 36,517 psi), while the elastic modulus decreased by less than 1% (from 4,320,000 psi to 4,310,000 psi). Increasing the length of the salt water exposure caused the tensile strength to drop by 25% (from 45,304 psi to 34,187 psi), and the elastic modulus to drop by 11% (from 4,320,000 to 3,860,000 psi). While these decreases appear rather large—especially the decrease in the tensile strength—the exposure conditions in the laboratory were much more severe than the deck would normally see in use since the in-service conditions would typically impose only intermittent exposure to salt water. In addition, the bridge deck was designed with a safety factor of 4 using conservative assumptions, providing sufficient material to offset these types of loss of strength.

Table 2. Test results, UVA-exposed coupons.

Part Identification	Ultimate Tensile Strength (psi)	Ultimate Tensile Strength Average (psi)	Ultimate Tensile Strength Std. Dev. (psi)	Elastic Modulus (psi)	Elastic Modulus Average (psi)	Elastic Modulus Std. Dev. (psi)
007 UVA	36,169.6	36,957.1	2,293.2	3,910,000	4,073,333.0	140,665.1
008 UVA	37,427.2			4,090,000		
009 UVA	38,218.3			4,060,000		
010 UVA	38,848.0			4,000,000		
011 UVA	38,392.0			4,330,000		
012 UVA	32,678.6			4,050,000		

Table 3. Test results, salt water coupons

Part Identification	Ultimate Tensile Strength (psi)	Ultimate Tensile Strength Average (psi)	Ultimate Tensile Strength Std. Dev. (psi)	Elastic Modulus (psi)	Elastic Modulus Average (psi)	Elastic Modulus Std. Dev. (psi)
001 (2 week)	37,153,8	36,517.6	818.4	4,180,000	4,310,000	225,167
002 (2 week)	35,594.3			4,180,000		
003 (2 week)	36,804.7			4,570,000		
004 (4 week)	34,552.0	34,187.7	2,744.2	3,770,000	3,860,000	155,885
005 (4 week)	31,279.5			3,770,000		
006 (4 week)	36,731.7			4,040,000		

3.2.1.2 Atmospheric coupons

The mass loss results for the atmospheric exposure coupons are shown in Table 4. With an average mass loss of 0.0243 mm/year, the data indicate that this location has low atmospheric corrosivity for steel. Given the location away from exposures to sea water and heavy industrial pollution, the reported results appear to be consistent with the relatively rural setting of the subject bridge. The coulometric reduction times for the silver coupons are shown in Figure 57, and the results are consistent with low levels of atmospheric chlorides that would be expected for this location. (All figures for this chapter appear immediately after the conclusion of the text.)

Table 4. Mass loss data

	Exposure Period	Pre-Weight (g)	Post-Weight (g)	Mass Loss (grams)	Corrosion Rate (mm/y)
Steel	3 months	29.8645	29.59235	0.27215	0.029205093
	6 months	31.0857	30.4063	0.6794	0.036454051
	9 months	30.8377	30.30647	0.53123	0.019002537
	12 months	30.3926	29.9291	0.4635	0.012434834
AL (AL2024 T3)	3 months	10.5001	10.28668	0.21342	0.064753481
	6 months	10.3794	10.3767	0.0027	0.000409602
	9 months	10.1385	10.13606	0.00244	0.000246772
	12 months	10.0519	10.0503	0.0016	0.000121363
AL (AL6061 T6)	3 months	5.9096	5.90549	0.00411	0.001283958
	6 months	5.9887	5.9849	0.0038	0.000593557
	9 months	6.1564	6.15079	0.00561	0.000584185
	12 months	6.3239	6.3212	0.0027	0.000210869
AL (AL7075 T6)	3 months	10.2416	10.07374	0.16786	0.050386443
	6 months	10.2273	10.2018	0.0255	0.00382716
	9 months	10.3593	10.2884	0.0709	0.007094004
	12 months	10.3452	10.3133	0.0319	0.002393851
Copper	3 months	34.6531	34.62201	0.03109	0.002933297
	6 months	34.3844	34.2857	0.0987	0.004656101
	9 months	34.407	32.9994	1.4076	0.044268345
	12 months	34.4875	34.3679	0.1196	0.002821022

3.2.1.3 Load testing

The onsite load testing was conducted on 25 March 2010 by Bridge Diagnostics, Inc. (BDI) of Boulder, CO. Strains were measured at 14 locations on the bridge, and displacements were measured at 9 locations on the deck and bridge structure. Examples of the sensor placement are shown in Figure 58 through Figure 60. A fully loaded dump truck weighing 78,660 lb was driven across the bridge at several lateral locations. The load test in progress is shown in Figure 61. BDI analyzed the data and determined that the maximum strain was in the range of 800–900 με, which is much less than the 3220 με limit. The maximum relative deck deflection (deflection of the deck with the girder deflection subtracted) was 0.14 in., which is less than the 0.16 in. requirement. The contractor's complete load test report was published in August 2016 as ERDC/CERL CR-16-3.

3.2.2 Inspections

On 4 November 2010, representatives from Mandaree Enterprise Corporation (MEC), ERDC-CERL, Redstone DPW, and Zellcomp met for discussion and to perform an inspection of the bridge. During the inspection, it quickly became apparent that water was being retained inside the channels of pultruded deck sections. This occurred because all of the weep holes were designed to be drilled in the bridge's easternmost edge, but

drainage through the half channels was interrupted by the grout pockets that had been created to encase the shear studs. As a consequence, any water that infiltrated the bridge deck “upstream” of these pockets was trapped by design. In addition, several weep holes had become plugged by concrete that escaped the barrier rail form facing the deck interior.

Because of the imminent onset of the winter freeze/thaw cycle in Huntsville, AL, immediate corrective action was undertaken to drill additional weep holes in the bottom of the deck. Overall, approximately 296 additional 0.5 in. diameter weep holes were drilled into the deck. Of those, approximately 90% drained in excess of 2 gallons of retained water (Figure 62). Finally, in locations where concrete was obstructing existing weep holes, MEC drilled replacement holes at higher elevations at 6 in. intervals until an unobstructed weep hole could be established (Figure 63).

In addition to finding retained water, the inspection confirmed the reflective cracking in the wear surface and the presence of voids in the grout haunch. The inspection also found that a significant amount of water was migrating through the grout haunch, particularly near voids, causing water to accumulate on girders and create corrosive conditions (Figure 64).

On 23 February 2011, MEC visited the bridge site to conduct a pre-repair survey to assess the extent of the voids in the haunch, test the inspection procedures, and plan the repair action. During this inspection, no water was observed on the girders in areas that had previously been wet, confirming the effectiveness of the added weep holes.

MEC also conducted a borescope inspection of the interior of several voids and several deck channels. During these inspections, no significant amount of water or external debris was observed in either the deck sections or in the voids. Figure 65 and Figure 66 show the interior of two voids. The bottom of the deck can be seen faintly at the top of each figure. Figure 67 and Figure 68 show the interior of composite deck sections. The deck surface and foam dam material for a grout pocket are visible.

3.2.3 Repairs to wear surface and voids

The bridge was closed to traffic for the duration of the repairs and material-curing intervals.

3.2.3.1 Wear surface and scuppers

Repairs to the wear surface and voids began 16 May 2011. First, dirt and other foreign materials were removed from the cracks adjacent to the raised flat composite sheets supporting the wear surface. The wear surface material was then removed to expose the closest fasteners (Figure 69). The exposed fasteners were removed to check whether the threads had damaged the composite material (Figure 70). Although not visible in Figure 70, in all cases the screws had in fact been overtightened, shearing the composite material and contributing to the panel raising. Replacement fasteners were installed adjacent to the original ones, and fasteners were added to help prevent any future panel lifting (Figure 71, Figure 72, and Figure 73). In all instances, replacing the fasteners returned the composite sheets to sit flush with the adjacent ones. Figure 73 shows two locations where extra screws were added before wear surface repair. The same area after the first application of polymer concrete is shown in Figure 74. The completed repair, before full cure, is shown in Figure 75.

After these initial repairs to the raised sheets and adjacent wear surfaces were finished, the reflective cracks were repaired. The cracks were cut open to provide a surface to adhere to the sealant. First, a straight cut was made to provide a guide for the second step (Figure 76), which was cutting a v-groove (Figure 77). The completed v-groove is visible in Figure 78. Once the v-groove was cut, the cracks were cleaned of dust and debris using compressed air. Next, a primer (Tremco Vulkem 171) was applied (Figure 79). This material was used at the suggestion of the sealant manufacturer because adhesion testing was not going to be practical for this particular repair, and the GFRP composite-sealant bond is not as common as bonds to other materials. Once the primer cured, the sealant (Tremco THC-901) was applied. The sealant was mixed in accordance with manufacturer's instructions, including the inclusion of a coloring agent to match the wear surface coloring. The sealant was applied with a bulk sealant gun (Figure 80). Before the sealant set, a scraper was used to remove excess material (Figure 81) and to ensure contact between the sealant bead and the top of the wear surface on each side of the joint (Figure 82). The completed repair is shown in Figure 83, and the procedure for the wear surface repair is documented in Appendix B, section B1.

Next, problems with the scuppers were addressed. During application of the wear surface, a polymer concrete lip, approximately 1/8 in. high, built up around the edge of the scuppers (Figure 84). The lips caused water to

pool on the bridge deck until it was deep enough to flow over into the scuppers (Figure 85). This drainage problem was compounded by the loose aggregate and sand that had migrated to the "downhill" side of the bridge. In order to facilitate drainage of the scuppers, these lips were removed using a grinder (Figure 86), and a slight downward bevel was ground toward the hollow of PVC body in each scupper (Figure 87). Completed repairs on the southwest end of the bridge can be seen in Figure 88. Note that a small fraction of the loose aggregate and sand that had accumulated on the bridge is visible in the upper left corner of Figure 88.

3.2.3.2 Voids in the grout

The first steps in repairing voids in the grout haunch were to identify and characterize them. A tap test was performed along the entire length of both sides of the two interior girders (Figure 89). A change in pitch of the resulting sound indicated the potential presence of a void. When a likely void was identified, caulk and backer rod were removed. The section was inspected visually (Figure 90) and probed with a thin metal rod. Some voids had to be confirmed with the borescope. Void width (across the girder), length (along the girder) and depth (above the girder) were determined, and the presence of water or external debris was noted. In all cases, the voids were free of external debris. The voids were free of detectable water except in one case, where a drain hole was drilled in the form plate, and a shop vacuum was used to remove any residual water.

Once the voids were identified, forms were attached to contain the repair material. First, mating surfaces on the bridge deck and steel grout haunch were mechanically cleaned using a scraper (Figure 91). Temporary forms to contain grout injected into the voids were fabricated from aluminum siding material bent to a right-angle profile. An injection hole was drilled in the "uphill" side of the form, where all of the voids were detected. In cases where the width of the void extended across the entire girder, aluminum containment forms were added to both sides of the girder, and a vent hole was drilled in the "downhill" side of the form in order to indicate the complete filling of the void and to avoid air entrapment. In cases where only one side of the girder allowed access to the void, vent holes were drilled on both sides of the injection hole to prevent air entrapment. In all cases, the mating surfaces for the aluminum containment forms were caulked using TremCo 626 sealant (Figure 92), and then the forms were

screwed into the bottom of the deck (Figure 93). Figure 94 shows the aluminum grout-containment form in place, drilled, and ready for grout injection.

The repair material (Euco Cable Grout PTX from Euclid Chemical) was prepared and mixed. The manufacturer's mix instructions were scaled down from construction quantities to produce enough grout to fill the bulk loading sealant gun used for the procedure. Grout was injected into the void through the injection hole (Figure 95) until it began to leak through the vent holes (Figure 96). After injection, the holes were plugged and the grout was allowed to set for at least 24 hours.

After the grout had set, the aluminum forms were removed (Figure 97) and the repair inspected. A repair immediately after form removal is shown in Figure 98. In three instances, the grout mixture was too thin and the aluminum forms failed to contain it. In these cases, the voids were re-formed, refilled, and allowed to cure for 24 hours. In all three cases, the second repair produced acceptable results. Once the repairs were inspected and accepted, excess caulk was removed (Figure 99), and any holes in the form plates were filled with caulk. The finished repair is shown in Figure 100.

This complete procedure is given in Appendix B, section B2.

3.2.3.3 Corrosion and further voids

During an inspection of the bridge in March 2012, areas of active corrosion were evident in places where the steel form for the grout haunch was attached to the top girder flange (Figure 101). Because the steel form provided no structural purpose after the grout haunch cured, sections affected by corrosion were cut out in order to evaluate the problem. As shown in Figure 102, red iron oxide corrosion had formed on the edge of the girder's top flange. When water is trapped behind inside the grout haunch form, this steel becomes electrochemically connected with the steel in the girders, evidently creating localized galvanic corrosion cells. To eliminate this condition, a contract was awarded through the Redstone DPW to remove the steel grout form from the entire bridge and to have the corroded areas of girder cleaned, surface-prepared, and painted.

The steel strips used to form the grout haunch were removed by grinding the welds with power tools. This operation revealed more voids in the

grout, especially along the inside surfaces of the two outermost girders (Figure 103). The previous tap tests had missed these voids, particularly in the same areas where concrete spilled from forms for the poured barrier rail.

At this point, a second contract was awarded to place grout into the newly discovered voids between the top girder flanges and the bottom of the composite deck. In some areas, contact between the grout and the composite deck was only about 50% effective. In preparation for new grout placement, the exposed areas along the top of the girder flanges were cleaned using power wire brushes and a high-pressure power washer. Then a primer coat of Sherwin Williams Zinc Clad II was applied. Euclid Cable Grout PXT, used in the previous procedure to fill voids, was applied to the areas with the missing grout. Initial use of a grout pump produced poor results. Subsequent application was done by hand packing. The water/cement ratio was reduced to produce a workable mix suitable for hand application. The edges were troweled to a neat straight line. After completing the grout placement, all exposed primed steel was coated with Sherwin Williams DTM B66 series acrylic finish coating.

3.3 Lessons learned

3.3.1 Technology installation

3.3.1.1 Grout haunch

Several factors are believed to have contributed to the voids present in the haunch. First, the manufacturer of the grout used (Euclid NS Grout from Euclid Chemical) requires that pea gravel aggregate be mixed into the grout for installations deeper than 2 in. The haunch for Bridge 18 has a minimum depth of 2.75 in., triggering this requirement. With the pea gravel included, the grout was much less flowable than it would have been otherwise, inhibiting the effective filling of the form.

This issue should be addressed in two ways. First, the depth of the haunch specified to support the GFRP composite deck should be designed to be less than 2 in. if possible. Second, the selected haunch material should be readily flowable and not require aggregate in order to reduce the formation of voids in the grout.

The second difficulty observed with the grout installation is that grout began leaking from the form (Figure 104) as soon as it had filled locally. Initially, this was seen as a good sign, as it demonstrated the form had been completely filled. However, the volume of grout that leaked was higher than initially believed, contributing to void formation. All observed voids were at locations where poor sealing could have contributed to leakage.

The sealing could be improved by building the haunch form from steel angles instead of straight plates. Angled forms would produce an area of overlap that would facilitate sealing.

The grout was hand-poured into the form from small buckets through the access holes in the composite deck (see Figure 23). This technique produced very little pressure to facilitate grout flow into and through the steel grout form welded to the girder web. The method could be improved by using a concrete pump or a purpose-built head box at the point of application for the grout.

After the grout pour was completed, the steel haunch form was left in place, recaulked where necessary, and painted to match the girders. This technique may be cosmetically appealing and could provide extra support to the bridge deck, but in practice it served to conceal the presence and extent of the voids until other signs prompted a careful investigation of the causes. Future GFRP bridge deck designs should include a drawing note that specifies removal of the forms and inspection of the haunch as soon as the grout has fully cured.

3.3.1.2 Bridge deck

Deck construction went smoothly, and the deck performed well after addressing minor issues related to installation of some components. First, the 3 in. diameter access holes used for welding the shear studs to the steel girders (see Figure 19) did not provide adequate clearance for the welder to weld the studs in the center of the hole (and thus the beam). Contractor personnel quickly learned that if the stud was centered in the 3-inch hole when welded, the gun had to be disassembled in order to remove it after welding a stud. Increasing the diameter of the access hole to 3.5 or 4 in. would provide clearance for welding gun. It would also provide flexibility when welding a shear stud onto a splice plate, where the fasteners also made it difficult to position shear studs. Increasing the size of the hole would also facilitate the flow of grout into the haunch form.

The lap joints between composite deck sections were initially designed to have fasteners driven through from the top side to the bottom of the deck. Inverting this approach (i.e., driving the fastener in from the bottom of the deck) results in an exposed fastener head rather than exposed threads, reducing the chances of injury due to accidental contact and also producing a more desirable appearance (see Figure 105).

Although the drainage holes were designed to be drilled in the lowermost side of the bridge deck to shed any water infiltrating the pultruded sections, the foam dams used to encase the shear studs while pouring the grout haunch allowed water to collect inside deck sections. Future applications of this system should be designed to provide drainage anywhere that water could infiltrate and become trapped.

In several instances, drain holes became partially obstructed due to debris or biological growth. In the future, the diameter of drain holes should be increased to facilitate drainage and decrease the likelihood of blockage.

3.3.1.3 GFRP composite top sheets

The only issue involving the composite top sheets, which provide the substrate for applying the polymer concrete wear surface, was lifting of edges observed in two places on the deck (see Figure 56). In both instances, the fastener head was recessed into the GFRP composite sheet, and removal of the fasteners from the sheets showed that the screw threads had pulled loose from the composite material. These facts suggest that the fasteners were overtightened, partially defeating panel attachment. In future installations, torque values for the fasteners should be specified to prevent overtightening.

3.3.1.4 Scuppers

At several visits to the bridge site, debris—mostly pine straw—was observed obstructing scuppers and impairing drainage. Larger-diameter scuppers would be less susceptible to such blockage, and should be specified in future applications.

The mild slope of this bridge, in combination with the tendency for road debris to accumulate on the side, makes it difficult for water to flow over the length of the bridge. This results in water not flowing all the way to the scuppers, which are located only at each end of the bridge. The result has

been puddling along the eastern edge of the bridge (see Figure 85), which may increase the probability of water infiltration into the deck. Adding scuppers along the length of the bridge would mitigate the problem.

Also contributing to the water pooling was the lip (Figure 84) that formed on the scuppers during installation of the wear surface. In future applications, installers should take care to make sure that the scupper threshold is not higher than the adjacent wear surface. As built, the scuppers on Bridge 18 protruded too much to accept water until the depth had reached approximately 1/8 in.

3.3.1.5 Wear surface

In 2007, a study of wear-surface materials applied to different composite bridge decks found that most had deteriorated to some degree [Ref. 16]. The study noted that the wear surfaces on most decks evaluated had deteriorated to some degree. The severity of the deterioration ranged from minor cracking to delamination of large portions of the wear surface.

The study identifies several potential causes of the wear surface deterioration. These include “several structural and environmental factors, e.g., poor adhesion, mismatch of coefficient of thermal expansion, and poor wear resistance at elevated temperatures” [Ref. 16].

Two specific material properties were identified as possibly contributing factors: coefficient of thermal expansion and modulus of elasticity. The study notes that composite materials frequently have much higher moduli than conventional wear surface materials. Specifically, “most polymeric materials have a relatively low and narrow ductile to brittle transition temperature” [Ref. 16].

Based on tests performed to evaluate the adhesion between wear surfaces and GFRP decking at various temperatures, the study concluded that the polymer concrete provides excellent adhesion to the GFRP material even without prior surface preparation.

This study also found that the material properties of the GFRP composite decking are more sensitive to changes in temperatures than the wear surface materials tested in the study. It was noted that even though “polymer concrete exhibits very good bond strength to GFRP surfaces, it is relatively stiff at low temperatures and creeps under wheel braking loads at elevated

temperatures. The fact that polymer concrete is stiff at low temperatures makes it susceptible to cracking over deck joints, particularly, under traffic loads" [Ref. 16]. That finding is consistent with observations of Bridge 18 made at Redstone Arsenal.

Finally, the study evaluated a hybrid wear surface option consisting of a 10 mm thick polymer concrete layer covered with a 40 mm thick layer of polymer-modified concrete. This surface takes advantage of good adhesion between itself and GFRP materials as well as the superior wear properties of polymer-modified concrete. Although the increased durability is appealing, it does not specifically address the tendency for reflective cracking. In fact, the study suggests that this surface material would conceal reflective cracks in the lower (polymer concrete) layer until they propagate through the polymer-modified concrete. This cracking would be more costly and difficult to repair than reflective cracking in a one-layer wear surface like the type demonstrated [Ref. 16].

The reflective cracking observed in the wear surface was perhaps the most serious issue affecting this technology. Although the deck is designed and tested to be stiff enough to prevent such cracking, in actual service cracking did occur. A number of factors are believed to have contributed to this, but it is impossible to determine with certainty why the cracking occurred to the extent observed.

Reflective cracking has also been observed in other bridges employing a GFRP deck and a polymer concrete wear surface. A high-stiffness (and, thus, low-deflection) design should not by itself be relied upon to be proof against cracking in service. A method of reducing the likelihood of reflective cracking would be to use fiberglass tape to bridge any gaps between the surface composite sheets, similar to how gypsum board is prepared before final surface preparation. This method could provide additional protection against reflective cracking in the event that deck deflection is greater than designed.

Another option would be to concede the fact that reflective cracking will occur and seal it preemptively. After the wear surface is installed and cured, the sealing procedures discussed in section 3.2.3.1 could be applied to provide a flexible seal wherever joints are likely to cause reflective cracking.

As designed and installed, the polymer concrete wear surface consists of one continuous sheet of material. Unless the coefficient of thermal expansion of the polymer concrete is exactly the same as the GFRP sheeting, a sufficiently large sheet will inevitably exhibit thermal deflection large enough to cause cracking. Future applications should have thermal expansion joints in the wear surface at appropriate intervals to prevent thermal cracking in the wear surface or delamination between the surface and composite sheets beneath it.

3.3.2 Operational lessons

The coarse aggregate used in the polymer concrete for this wear surface tends to trap debris, especially in non-traffic areas. At present, debris (primarily loose aggregate and sand) has accumulated along the eastern edge of the bridge. This debris inhibits water flow to the ends of the bridge and, thus, the scuppers. Because this problem contributes to the puddling observed in Figure 85, road maintenance personnel should periodically clear accumulated debris to avoid drainage problems.

3.4 Figures for Chapter 3

Figure 57. Coulometric reduction times for silver coupons.

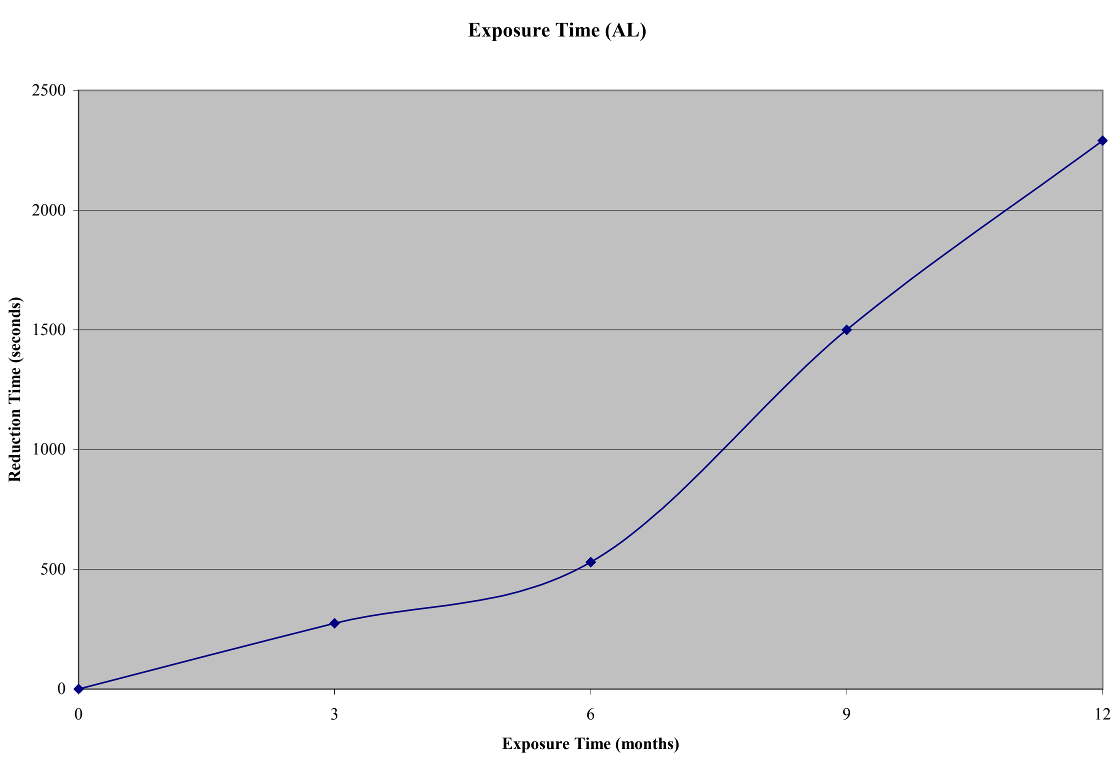

Figure 58. Strain and displacement gauges placed for onsite load testing.

Figure 59. Displacement gauges on bottom of bridge deck.

Figure 60. Displacement and strain gauges on bottom of girder.

Figure 61. Vehicle used for onsite load test.

Figure 62. Water draining from additional weep holes.

Figure 63. Additional weep hole drilled next to concrete-obstructed hole.

Figure 64. Moisture infiltrated through grout onto girder.

Figure 65. Borescope view of void interior.

Figure 66. Borescope view of void interior.

Figure 67. Borescope view of deck section interior.

Figure 68. Borescope view of deck section interior.

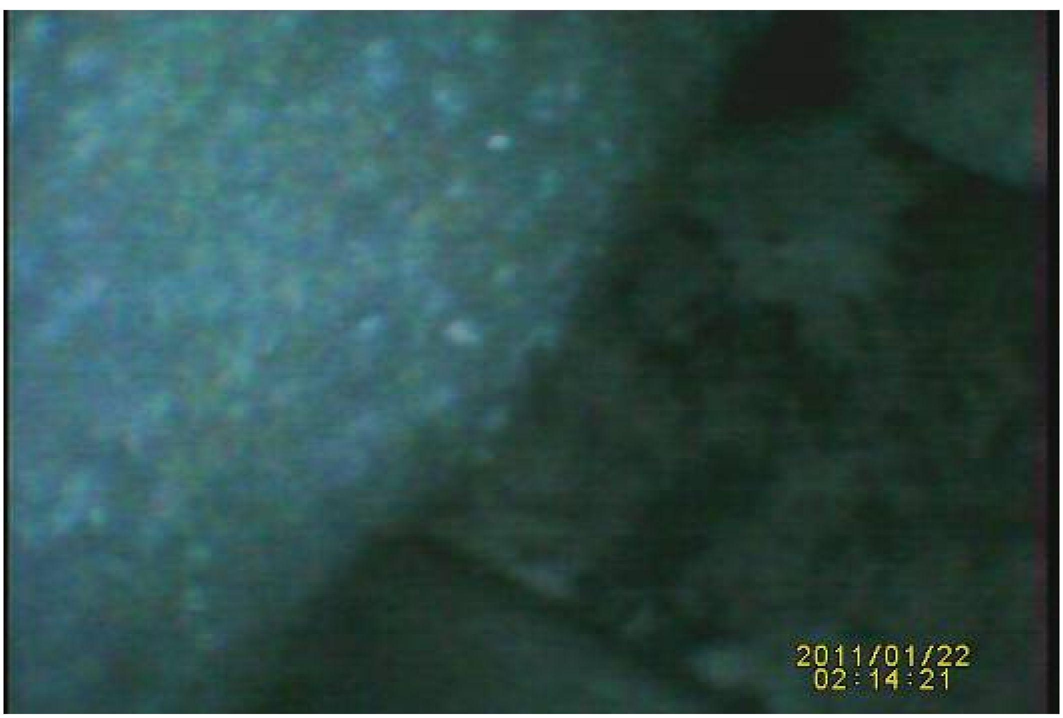

Figure 69. Wear surface hole and gap between GFRP composite sheets.

Figure 70. Fastener removed from GFRP composite sheet.

Figure 71. GFRP composite sheets with additional fasteners installed.

Figure 72. GFRP composite sheets with additional fasteners installed.

Figure 73. GFRP composite sheets with additional fasteners installed.

Figure 74. Patched areas of wear surface.

Figure 75. Completed polymer concrete hole repair prior to full cure.

Figure 76. Straight cut with guide chalk line.

Figure 77. Cutting v-groove.

Figure 78. V-groove in wear surface.

Figure 79. Primer application.

Figure 80. Application of wear surface sealant.

Figure 81. Removal of excess sealant material.

Figure 82. Smoothing excess sealant material.

Figure 83. Completed wear surface sealing.

Figure 84. Polymer concrete lip around scupper.

Figure 85. Water pooling on bridge.

Figure 86. Grinding lip off scupper.

Figure 87. Repaired scupper.

Figure 88. Repaired scuppers.

Figure 89. Tap test.

Figure 90. Void inspection.

Figure 91. Cleaning surfaces prior to attaching grout form.

Figure 92. Caulking form joints.

Figure 93. Drilling pilot holes for form attachment.

Figure 94. Attached form with injection hole.

Figure 95. Grout injection.

Figure 96. Back-side form with leaking grout.

Figure 97. Form removal.

Figure 98. Raw repair after form removal.

Figure 99. Repair finishing.

Figure 100. Finished repair.

Figure 101. Corrosion on top flange where steel strip attached to form grout haunch.

Figure 102. Exposed area after the steel strip peeled back.

Figure 103. Extensive missing grout revealed after steel strips removed.

Figure 104. Grout leaking through caulk.

Figure 105. Lap joint showing inverted fastener.

4 Economic Summary

4.1 Costs and assumptions

Total cost for the execution of this demonstration project (including, design, manufacturing, program management, installation, and required post-installation repairs of the composite deck technology) was $918,000. The GFRP composite deck is assumed to have a 75-year life.

The estimated construction cost for a steel-reinforced concrete bridge deck was obtained by calculating the square footage of the bridge replaced in the project. This was determined to be 4,518 sq ft (198 ft, 7 in. by 22 ft, 9 in.). This area was multiplied by the following factors: $12.40/sq ft for demolition and disposal, $42.00/sq ft for construction of a steel-reinforced deck, and $24.00/sq ft for traffic control. These calculations produced an estimated cost of $354,211 for a steel-reinforced concrete deck equivalent to the deck installed in this demonstration.

Actual costs for design, manufacturing, demolition, and traffic control were used for the GFRP deck. The cost of the installation contractor was $150,339, and included demolition/disposal, construction, and traffic control. The deck manufacturer's costs was estimated to be $379,129, including materials, engineering, overhead, and profit. The manufacturer's travel for the one-time installation to support the project-specific requirements were removed to arrive at this figure. Overall, the cost of a composite bridge deck was calculated to be $529,468.

For purposes of the economic analysis, replacement was assumed to be necessary for 30 bridges at Redstone Arsenal. The first composite bridge deck was installed in Year 1 as part of the present project, and five additional composite bridge deck installations were assumed for each year after that, with four bridges rehabilitated with a composite deck in Year 7 for a total of 30. For the conventional reinforced concrete deck, replacement of five bridges per year is assumed starting in Year 1. Thirty concrete bridge decks will be replaced by Year 6. With an average 25-year life expectancy, the replacement cycle for the concrete decks will start again in Year 26.

The reinforced-concrete deck was assumed to require pothole repairs totaling $5,000 per bridge per year. In the first six years, the bridges with

newly replaced decks will not require pothole repair in their first year. In addition, the concrete bridge decks were assumed to require replacement of their expansion joints every five years. Decks were assumed to have a 22.75 ft width and to require five expansion joints (joints at both ends of the bridge plus three between the four spans of the bridge). A cost of $55 per linear foot of joint was used, producing an estimated total of $6,256 per bridge. Replacement of expansion joints starts in Year 1, assuming repair of existing bridges. No maintenance is assumed to be necessary for the composite deck over the thirty-year analysis period.

In addition to the maintenance savings, traffic control costs of $0.96/day/sq ft were assumed. The annual pothole maintenance was assumed to take three days at $2.88/sf, resulting in a cost of $13,012 per bridge. In addition, the expansion joint maintenance (which will occur every five years) was also assumed to require three days of traffic control, and results in identical costs.

4.2 Projected return on investment (ROI)

Using data generated from this project and methods prescribed by the Office of Management and budget [Ref. 17], the 30-year ROI for this project was calculated to be 6.4, as compared to the originally estimated ROI of 9.9. That original ROI estimate had all 30 bridges replaced in Year 1, with the concrete bridge decks replaced after 15 years instead of 25. Since the replacement of all 30 bridges in Year 1 was considered unrealistic, the revised assumptions given above were used in the recalculation. If pothole repairs and joint repairs were done at the same time, the baseline traffic costs would be reduced slightly, and those savings would account for a slightly lower and more conservative ROI of 5.4. See Table 5 for the recalculations using values and data generated by the demonstration.

Table 5. Thirty-year ROI for demonstrated technology.

Return on Investment Calculation

Investment Required				918,000
Return on Investment Ratio	5.40		Percent	540%
Net Present Value of Costs and Benefits/Savings	11,463,141		16,418,847	4,955,706

A Future Year	B Baseline Costs	C Baseline Benefits/Savings	D New System Costs	E New System Benefits/Savings	F Present Value of Costs	G Present Value of Savings	H Total Present Value
1	2,252,635					2,105,313	2,105,313
2	2,252,635		2,647,340		2,312,187	1,967,451	-344,735
3	2,252,635		2,647,340		2,161,024	1,838,826	-322,198
4	2,252,635		2,647,340		2,019,656	1,718,535	-301,120
5	2,252,635		2,647,340		1,887,553	1,606,129	-281,425
6	2,252,635		2,647,340		1,763,923	1,500,931	-262,992
7	577,896		2,117,872		1,318,799	359,856	-958,943
8	577,896					336,335	336,335
9	577,896					314,318	314,318
10	577,896					293,745	293,745
11	577,896					274,558	274,558
12	577,896					256,586	256,586
13	577,896					239,827	239,827
14	577,896					224,108	224,108
15	577,896					209,430	209,430
16	577,896					195,733	195,733
17	577,896					182,962	182,962
18	577,896					170,999	170,999
19	577,896					159,788	159,788
20	577,896					149,328	149,328
21	577,896					139,562	139,562
22	577,896					130,431	130,431
23	577,896					121,878	121,878
24	577,896					113,903	113,903
25	577,896					106,448	106,448
26	2,252,635					387,904	387,904
27	2,252,635					362,449	362,449
28	2,252,635					338,796	338,796
29	2,252,635					316,720	316,720
30	2,252,635					295,996	295,996

5 Conclusions and Recommendations

5.1 Conclusions

Although there were several problems during this demonstration with the installation of the pultruded composite bridge deck at Redstone Arsenal, the results demonstrate that this technology can be implemented to rehabilitate properly selected reinforced concrete vehicle bridges at reduced life-cycle cost. The use of composite deck components eliminates the vulnerability to structural problems associated with the corrosion of reinforcing steel in conventional vehicle bridges located in corrosive environments. Additionally, load testing results indicate that this technology could be used to extend the service life of old, deteriorated steel bridges because of increases in the strength-to-weight ratio achieved by using GFRP composites versus reinforced concrete for deck replacement. With minor changes made to bridge design and construction processes, GFRP composite decks could be implemented reliably in a variety of situations.

The main performance concern with the technology in this demonstration was wear-surface cracking, although this problem can likely be addressed through further improvements in methods and materials as the technology is applied more widely. By comparison, problems such as deck cracking and potholes are common and universal in reinforced concrete bridge decks due to reinforcement bar corrosion as aggravated by loading, weathering, and chloride intrusion.

5.2 Recommendations

5.2.1 Applicability

For maximum life-cycle cost benefit, this technology should be deployed in high-corrosion areas such as a coastal region with high atmospheric chloride content and humidity. Composite decks could also provide significant benefits when incorporated into the design of movable bridges (e.g., a drawbridge or swinging bridge) to take advantage of their superior strength-to-weight ratio as compared with reinforced concrete decks. This strength-to-weight benefit also makes composite decks a good candidate technology for refurbishing aged bridges where degradation of the superstructure has reduced load-carrying capacity.

Another advantage this technology offers is a faster construction process. With sufficient planning and experience, a deck similar to the one demonstrated in this project could be built very quickly. The limiting factor would be cure time for the grout haunches, barrier rails, and wear surface. This technology should be fully considered in situations where a bridge deck must be replaced while alternative approaches are unavailable or impractical from an engineering standpoint.

5.2.2 Implementation

According to Unified Facilities Criteria (UFC) 3-301-01, *Structural Engineering* [Ref. 18], highway bridges shall be designed in accordance with AASHTO HS-20, "LRFD (Load and Resistance Factor Design) Bridge Design Specifications" [Ref. 3] and Volume 4, "Structural Behavior of Steel" in the FHWA *Steel Bridge Design Handbook* [Ref. 20]. There is an AASHTO specification for GFRP-reinforced concrete bridge decks and traffic railings [Ref. 19], but it does not cover composite bridge decking. AASHTO Subcommittee T-6, Fiber Reinforced Polymer Composites, is aware of this technology but, at present, composite vehicle decks are considered a niche product with limited application beyond movable bridges and older truss bridges. With few suppliers and little current interest from state departments of transportation, the development of AASHTO guidance is presumably many years away. However, as validated in this demonstration, AASHTO specifications can be applied in conjunction with manufacturer guidance to successfully implement the technology.

There also is currently no guidance in any Unified Facilities Criteria (UFC) or Unified Facilities Guide Specification (UFGS) documents on GFRP composite bridge decks. Under a project funded in Fiscal Year 2015, ERDC-CERL is developing a new UFC for the use of GFRP composites in bridge structures, including decks. Publication of the UFC is expected in early 2017. This guidance is expected to facilitate the use of GFRP composites for bridges in advance of AASHTO guidance.

5.2.3 Future monitoring at demonstration site

Because the durability of the wear surface was the greatest concern in this project, the Redstone bridge rehabilitated in this demonstration should continue to be monitored to evaluate its long-term performance under installation traffic and weather conditions. Similarly, other applications of this GFRP composite bridge deck technology on DoD properties should be

investigated to determine whether similar results have been noted. Findings from periodic monitoring and inspections could impact future guidance revisions.

References

1. FHWA RD-01-156. 2002. *Corrosion Costs and Preventive Strategies in the United States*. Washington, DC: U.S. Department of Transportation, Federal Highway Administration.

2. Hastak, M., D. Halpin, and T. Hong. November 2004. "Constructability, Maintainability, and Operability of Fiber Reinforced Polymer (FRP) Bridge Deck Panels." Joint Transportation Research Program, Project No. C-36-56NNN (FHWA/IN/JTRP-2004/15). West Lafayette, IN: Purdue University.

3. AASHTO HS-20. 2007. *Load and Resistance Factor Design: LRFD Bridge Design Specifications*, 4th edition. Washington D.C.: American Association of State Highway and Transportation Officials.

4. Alabama Department of Transportation (ALDOT). 1 January 2008. *ALDOT Bridge Bureau Structures Design and Detailing Manual*. Standard Drawing I-131. Montgomery, AL: ALDOT Bridge Bureau.

5. ASTM Standard A493-09. 2009. *Standard Specification for Stainless Steel Wire and Wire Rods for Cold Heading and Cold Forging*. DOI: 10.1520/A0493-09. West Conshohocken, PA: ASTM International.

6. ASTM Standard A709-11. 2011. *Standard Specification for Structural Steel for Bridges*. DOI: 10.1520/A0709_A0709M-11. West Conshohocken, PA: ASTM International.

7. ASTM Standard A123-09. 2009. *Standard Specification for Zinc (Hot-Dip Galvanized) Coatings on Iron and Steel Products*. West Conshohocken, PA: ASTM International. doi: 10.1520/A0123_A0123M-09.

8. ASTM D790-10. 2010. *Standard Test Method for Flexural Properties of Unreinforced and Reinforced Plastics and Electrical Insulating Materials*. West Conshohocken, PA: ASTM International. doi: 10.1520/D0790-10.

9. ASTM D638-10. 2010. *Standard Test Method for Tensile Properties of Plastics*. West Conshohocken, PA: ASTM International. doi: 10.1520/D0638-10.

10. ASTM G151-12. 2012. *Standard Practice for Exposing Nonmetallic Materials in Accelerated Test Devices that Use Laboratory Light Sources*. West Conshohocken, PA: ASTM International. doi: 10.1520/G0151-12.

11. ASTM G154-12. 2012. *Standard Practice for Operating Fluorescent Ultraviolet (UV) Lamp Apparatus for Exposure of Nonmetallic Materials*. West Conshohocken, PA: ASTM International. doi: 10.1520/G0154-12.

12. ASTM D4329-13 2013. *Standard Practice for Fluorescent Ultraviolet (UV) Lamp Apparatus Exposure of Plastics*, Procedure 7.2.2, Cycle B. West Conshohocken, PA: ASTM International. doi: 10.1520/D4329-13.

13. ASTM D3039-08. 2008. *Standard Test Method for Tensile Properties of Polymer Matrix Composite Materials*. West Conshohocken, PA: ASTM International. doi: 10.1520/D3039-08.

14. ASTM G1-03. 2003. *Standard Practice for Preparing, Cleaning, and Evaluating Corrosion Test Specimens*. West Conshohocken, PA: ASTM International. doi: 10.1520/G0001-03.

15. ASTM Standard B825-08. 2008. *Standard Test Method for Coulometric Reduction of Surface Films on Metallic Test Samples*. West Conshohocken, PA: ASTM International. doi: 10.1520/B0825-02R08.

16. Aboutaha, Riyad S. 2007. "Innovative Hybrid Wearing Surfaces for FRP Bridge Decks." Presented at the 16th International Conference on Composite Materials (ICCM-16), Kyoto, Japan, July 8–13.

17. Office of Management and Budget (OMB). 1992. *Guidelines and Discount Rates for Benefit-Cost Analysis of Federal Programs*. OMB Circular No. A-94. Washington, DC: Office of Management and Budget.

18. Unified Facilities Criteria (UFC) 3-301-01. June 2013. *Structural Engineering*. Washington DC: Department of Defense.

19. AASHTO. 2009. *LRFD Bridge Design Guide Specifications for GFRP-Reinforced Concrete Bridge Decks and Traffic Railings*. Washington D.C.: American Association of State Highway and Transportation Officials.

20. FHWA. December 2015. "Structural Behavior of Steel." Volume 4 of *Steel Bridge Design Handbook* (19 volumes). Publication No. FHWA-HIF-16-002. Washington, DC: U.S. Department of Transportation, Federal Highway Administration.

Appendix A: Material Testing Results

A1. Initial testing by manufacturer

Creative Pultrusions
Quality Assurance
Test Summary Report

Part Id:	CP216.102		Date Tested:		December 21, 2009	
Description:	7" Bridge Deck		Date Produced:		December 18, 2009	
Production Order:						
Mechanical Properties						
	ASTM	Results			Minimum	
	Test	Average	Std. Dev.	Units	Required	
Tensile Strength Lengthwise	D638	45,304	2,685	psi		
Tensile Modulus Lengthwise	D638	4.32E+06	2.37E+05	psi		
Flexural Strength Lengthwise	D790	44,760	3,113	psi		
Flexural Modulus Lengthwise	D790	2.78E+06	2.31E+05	psi		

See Drawing below for sample location.

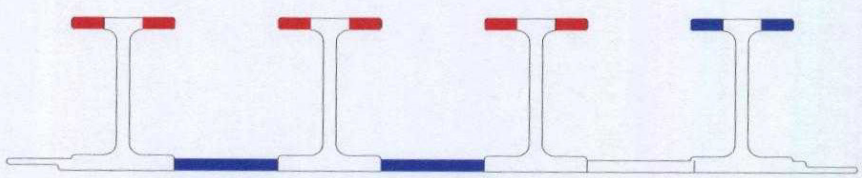

Red= Tensile Location
Blue= Flexural Location

Tested By: D. Crawford
Quality Assurance Specialist

Approved By: D. Allison
Quality Assurance Supervisor

A2. Testing by independent laboratory

APPLIED TECHNICAL SERVICES, INCORPORATED

1049 Triad Court, Marietta, Georgia 30062 • (770) 423-1400 Fax (770) 424-6415

MATERIALS TEST REPORT

Ref. D149095 **Date** May 25, 2010 **Page** 1 **of** 2

Purchase Order #: W9132T-ATS-001-01

Karl Palutke
Mandaree Enterprise Corp.
812 Park Drive
Warner Robins, Georgia 31088

Test Procedure

Test Performed	Test Procedure
Tensile	ASTM D 3039-08

Test Material	Conditioning
Composite Bridge Materials	UV Exposure per ASTM G 154 (2,000 Hrs.)

Test Results

Part Identification	Ultimate Tensile Strength			Elastic Modulus		
	(PSI)	Average (PSI)	Std. Dev. (PSI)	(PSI)	Average (PSI)	Std. Dev. (PSI)
007 UV	36,169.6	36,957.1	2,293.2	3,910,000	4,073,333.0	140,665.1
008 UV	37,427.2			4,090,000		
009 UV	38,218.3			4,060,000		
010 UV	38,848.0			4,000,000		
011 UV	38,392.0			4,330,000		
012 UV	32,687.6			4,050,000		

ISO 9001

Prepared by: J. Kimble
Materials Testing

Approved by: E. Sproat
Materials Testing

ATS 904, 01/2010

APPLIED TECHNICAL SERVICES, INCORPORATED

1049 Triad Court, Marietta, Georgia 30062 • (770) 423-1400 Fax (770) 424-6415

MATERIALS TEST REPORT

Ref. D149095 **Date** May 25, 2010 **Page** 2 **of** 2

Purchase Order #: W9132T-ATS-001-01

Karl Palutke
Mandaree Enterprise Corp.
812 Park Drive
Warner Robins, Georgia 31088

Test Procedure

Test Performed	Test Procedure
Tensile	Customer Spec.

Test Material	Conditioning
Composite Bridge Materials	Salt Water Exposure (2 & 4 Week Expsoure)

Test Results

Part Identification	Ultimate Tensile Strength			Elastic Modulus		
	(PSI)	Average (PSI)	Std. Dev. (PSI)	(PSI)	Average (PSI)	Std. Dev. (PSI)
001 (2 Week)	37,153.8	36,517.6	818.4	4,180,000	4,310,000	225,167
002 (2 Week)	35,594.3			4,180,000		
003 (2 Week)	36,804.7			4,570,000		
004 (4 Week)	34,552.0	34,187.7	2,744.2	3,770,000	3,860,000	155,885
005 (4 Week)	31,279.5			3,770,000		
006 (4 Week)	36,731.7			4,040,000		

ISO 9001

Prepared by: J. Kimble
Materials Testing

Approved by: E. Sproat
Materials Testing

ATS 904, 01/2010

Appendix B: Contractor Repair Procedures

B1. Wear surface repair procedures

1. The contractor shall saw a straight cut over existing cracks (and existing panel joints), approximately 965 linear feet. The width of the cut shall not exceed 1/8 in.
2. Upon completion of the straight line cut, contractor shall cut a v-groove following the initial straight line cut. The depth of the v-groove shall be deep enough to expose the FRP panels underneath the wear surface, but shall not exceed 9/16 in. in depth without MEC concurrence. The v-cut shall not extend more than 1/4 in. into the FRP material. The width of the groove shall not exceed the groove's depth.
3. After completion of the v-groove, all joints shall be cleared of dust, debris, and moisture using compressed air and, if necessary, manual sweeping/wiping.
4. Following cleaning, all joints will be treated with TremCo 171 Primer. NOTE: this operation shall not be performed if dust, debris, or moisture is present in the cut, or if the ambient temperature is below 72 °F. Primer shall be allowed to cure overnight prior to sealing.
5. After priming, all joints shall be filled using Vulkem THC 901 sealant, mixed or dyed to approximate the color of the wear surface. NOTE: this operation shall not be performed if dust, debris, or moisture is present in the cut, or if the ambient temperature is below 72 °F.
6. After joint filling, sealant shall be manually spread in order to guarantee contact with the wear surface on both sides of the joint.
7. Sealant shall be allowed to set for 72 hours prior to exposure to vehicular traffic.

B2. Grout haunch void-filling procedures

Step 1–Identify/characterize voids

To identify voids in the grout trough, MEC will perform a tap test and listen for changes in pitch of the resulting sound. When a potential void is identified, MEC will remove all backing cord between the bridge deck and the form plate welded to the top of the girders for retaining the grout. All areas of visible voids will be probed between the form plate and the bridge deck to determine if a void exists and if so, the size of the void. In addition, MEC will devote additional attention to areas on the girders that appear to be accumulating moisture. This attention will include drilling inspection

holes through the form plate in areas where there is a presence of moisture or the tap tests indicate a possible void.

Once a void is identified, MEC will use metallic probes and a fiber optic borescope to characterize the void. The void width (along the girder), depth (across the girder), and the void space in the haunch area will be determined as best as will be possible. Based on this information, MEC will decide the most appropriate means of removing standing water, if any, from the void. If the height of the void is such that the bottom surface of the void is significantly below the bottom edge of the gap between the plate and the bridge deck, MEC will drill a drain hole to facilitate drainage. For voids where bottom surface of the void is close to the bottom of the gap, the void will be dried manually using towels forced through the gap and then removed. Forced air will also be considered depending on the circumstance.

Step 2–Forming

Depending on the size of the gap between the steel plate and the bottom of the bridge deck, MEC will decide if additional forming is necessary to contain the grout. If so, right-angle forming will be added to seal the gap. The angle will be attached to the bottom of the deck using self-tapping screws and will be sealed to the side of the form plate using TremPro 626 Polyurethane Sealant.

For shallow voids (voids that don't extend lower than the top of the gap between the plate and the bottom of the bridge deck), an injection hole will be drilled in the form plate (or in the right-angle form, if appropriate) in line with the center of the void, with vent holes drilled every six inches along the rest of the length of the void. For voids that extend through the width of the girder to the other edge, vent holes will be drilled on the opposite side of the girder as well. This will inhibit air entrapment and also provide visual feedback that the void has been filled from grout exuding from the holes.

Step 3–Mixing/injection

MEC will mix replacement grout (Euclid Euco Cable Grout PTX – a low-viscosity grout formulated for easy pumping) in a fluid consistency in accordance with the manufacturer's instructions (1.5–1.7 gal of water for 50 lb of dry grout for a fluid consistency). The grout will be injected using

a caulk-gun-like apparatus (Cox 51002 Portland 34 oz Manual Bulk Applicator) capable of loading and injecting bulk materials. Grout will be injected until its presence is detectable at all drain/vent holes. As grout is detected draining from the vent holes, they will be plugged temporarily. Upon completion of grout injection, the injection hole will be plugged temporarily to prevent the grout from escaping. Once the grout has reached its initial set, the temporary plugs will be removed. The metal surrounding the holes will be cleaned, and (if necessary) its coating will be touched up to prevent corrosion. Once the touch-up is complete, the holes will be sealed.

If a form was required, it will be left in place a minimum of 12 hours after grout injection (grout reaches initial set in 8–10 hours, according to the manufacturer).

Step 4–Cleanup

After the grout has been allowed to set for 12 hours, any forms will be removed and the grout will be inspected. All backing cord will be replaced, and other seams will be sealed.

Step 5–Caulking joints in form plate after repairs

1. Clean the surface of the form plate. Any dirt or corrosion product will be removed using a scraper or stiff-bristled brush. After brushing, the surface will be wiped clean with a clean rag.
2. Touch up the surface with a cold galvanizing compound as required.
3. Apply backing cord or TremPro 626 Polyurethane Sealant to joints of form plates.
4. Paint all sealed areas with sprayable cold galvanizing compound from Zinga Industries.

REPORT DOCUMENTATION PAGE

Form Approved
OMB No. 0704-0188

1. REPORT DATE *(DD-MM-YYYY)*
August 2016

2. REPORT TYPE
Final

3. DATES COVERED *(From - To)*

4. TITLE AND SUBTITLE
Demonstration and Validation of a Lightweight Composite Bridge Deck Technology as an Alternative to Reinforced Concrete: Final Report on Project F09-AR16

5a. CONTRACT NUMBER

5b. GRANT NUMBER

5c. PROGRAM ELEMENT NUMBER
Corrosion Prevention and Control

6. AUTHOR(S)
Karl Palutke, Richard G. Lampo, Lawrence Clark, James Wilcoski, Rick Miles, and Darrel Skinner

5d. PROJECT NUMBER
F09-AR16

5e. TASK NUMBER

5f. WORK UNIT NUMBER

7. PERFORMING ORGANIZATION NAME(S) AND ADDRESS(ES)
U.S. Army Engineer Research and Development Center
Construction Engineering Research Laboratory
P.O. Box 9005
Champaign, IL 61826-9005

8. PERFORMING ORGANIZATION REPORT NUMBER
ERDC-CERL TR-16-16

9. SPONSORING / MONITORING AGENCY NAME(S) AND ADDRESS(ES)
Office of the Secretary of Defense
3090 Defense Pentagon
Washington, DC 20301-3090

10. SPONSOR/MONITOR'S ACRONYM(S)
OUSD(AT&L)

11. SPONSOR/MONITOR'S REPORT NUMBER(S)

12. DISTRIBUTION / AVAILABILITY STATEMENT
Approved for public release; distribution is unlimited.

13. SUPPLEMENTARY NOTES

14. ABSTRACT
Cyclic loading and weathering of reinforced concrete bridge decks cause corrosion of reinforcement steel, which leads to cracking, potholes, and other problems. This project demonstrated the use of a glass-fiber reinforced polymer (GFRP) composite deck system, which does not use any reinforcement steel, on a deteriorated concrete bridge at Redstone Arsenal, AL. A pultruded deck system made by Zellcomp, Inc., was selected for demonstration and validation. The demonstrated system was designed to retain the 36-ton (HS-20) load rating of the original bridge. This report documents demolition of the existing deck, installation of the composite deck system, materials and load testing, remediation of initial problems, and an economic analysis in terms of return on investment (ROI).

The main problems identified after construction were reflective cracking of the polymer-concrete wear surface applied over the composite deck sections; and gaps and voids related to grout forms and supports installed between bridge girders and deck sections. After repairs, the bridge was returned to service and is functioning normally. The calculated ROI for this technology was 5.4. Although there are not yet consensus standards for composite bridge decks, the demonstrated technology can be effectively applied using existing load-resistance design factors and manufacturer installation instructions.

15. SUBJECT TERMS
glass fibers; concrete–service life; concrete bridges–floors; polymeric composites; fibrous composites; concrete bridges–maintenance and repair

16. SECURITY CLASSIFICATION OF:			17. LIMITATION OF ABSTRACT	18. NUMBER OF PAGES	19a. NAME OF RESPONSIBLE PERSON
a. REPORT	**b. ABSTRACT**	**c. THIS PAGE**			**19b. TELEPHONE NUMBER *(include area code)***
Unclassified	Unclassified	Unclassified	UU	106	

Standard Form 298 (Rev. 8-98)
Prescribed by ANSI Std. 239.18